Original Research

Astragaloside IV inhibits renal tubulointerstitial fibrosis by blocking TGF-β/Smad signaling pathway *in vivo* and *in vitro*

Li Wang[1], Yang-Feng Chi[2], Ze-Ting Yuan[3], Wen-Chao Zhou[1], Pei-Hao Yin[2], Xue-Mei Zhang[4], Wen Peng[1,2] and Hui Cai[5,6]

[1]Laboratory of Renal Disease, Putuo Hospital, Shanghai University of Traditional Chinese Medicine, Shanghai 200062, China; [2]Department of Nephrology, Putuo Hospital, Shanghai University of Traditional Chinese Medicine, Shanghai 200062, China; [3]Experimental Research Center, Putuo Hospital, Shanghai University of Traditional Chinese Medicine, Shanghai 200062, China; [4]Department of Pharmacology, School of Pharmacy, Fudan University, Shanghai 201203, China; [5]Renal Division, Department of Medicine, Emory University School of Medicine, Atlanta, GA 30322, USA; [6]Section of Nephrology, Atlanta Veterans Administration Medical Center, Decatur, GA 30322, USA

Xue-Mei Zhang and Wen Peng are co-corresponding authors.

Corresponding author: Wen Peng. Email: pengwen_01@vip.sina.com; Xue-Mei Zhang. Email: xuemzhang@fudan.edu.cn

Abstract

Astragaloside IV (AS-IV) is a major active ingredient from *Radix astragali*, which has been considered as a renoprotective agent; however, its molecular mechanisms are unclear. Thus, we designed to investigate the renoprotective effects and mechanisms of AS-IV in rat model of renal fibrosis induced by unilateral ureteral obstruction (UUO) *in vivo* and TGF-β1-stimulated rat renal fibroblasts (NRK-49F) *in vitro*. Sprague-Dawley rats were randomly divided into six groups: sham operation, UUO, UUO/AS-IV (3.3, 10, 33 $mg \cdot kg^{-1} \cdot d^{-1}$), and UUO/enalapril (4 $mg \cdot kg^{-1} \cdot d^{-1}$). Renal function, tubulointerstitial damage index score, extracellular matrix (ECM) deposition, and the expressions of TGF-β1, connective tissue growth factor (CTGF), α-SMA, fibronectin, collagen I, III, Smad2/3, phosphorylated-Smad2/3, and Smad7 were measured. In addition, the expressions of CTGF, α-SMA, fibronectin, collagen I, III, Smad2/3, phosphorylated-Smad2/3, and Smad7 were measured in TGF-β1-stiumlated NRK-49F cell line. AS-IV significantly decreased UUO-induced renal fibrosis and functional impairment, which are associated with inhibition of TGF-β1, CTGF, α-SMA, and collagen matrix expression, and a decrease in serum creatinine and urea nitrogen. The renoprotective effects of AS-IV on fibrosis were associated with up-regulation of Smad7, thereby blocking up-regulations of TGF-β1, CTGF, and α-SMA, and activation of phosphorylated-Smad2/3. These effects were further conformed in NRK-49F cell line stimulated by TGF-β1. Moreover, knockdown of *Smad7* gene in NRK-49F cells was able to prevent AS-IV-induced inhibition to Smad2/3 signaling activation, expression of CTGF, α-SMA, and ECM proteins in response to TGF-β1. Renal tubulointerstitial fibrosis was attenuated by treatment with AS-IV, which was closely related to induction of Smad7, thereby inhibiting TGF-β/Smad signaling.

Keywords: Astragaloside IV, renal tubulointerstitial fibrosis, unilateral ureteral obstruction, TGF-β/Smad signaling pathway

***Experimental Biology and Medicine* 2014; 239: 1310–1324. DOI: 10.1177/1535370214532597**

Introduction

Renal fibrosis is characterized by the accumulation of fibroblasts and the excessive extracellular matrix (ECM) that replaces normal kidney structure irrespective of the initiating pathology.[1] Tubulointerstitial fibrosis is considered as the final common pathway for all chronic kidney diseases (CKDs).[2] Recent studies have demonstrated that a key step in tubulointerstitial fibrosis is epithelial-mesenchymal transition (EMT), a process whereby fully differentiated epithelial cells undergo transition to mesenchymal phenotype.[3,4] EMT causes a substantial increase in the number of myofibroblasts that contributes to the development of progressive renal fibrosis.[5] Thus, inhibiting myofibroblast accumulation is critical in preventing tubulointerstitial fibrosis and preserving renal function.

Injury to the kidney is associated with the release of cytokines/growth factors such as TGF-β, epithelial growth factor (EGF), and platelet-derived growth factor (PDGF) by damaged or infiltrating cells. An increase in production of TGF-β is one of the most important mechanisms in the pathogenesis of renal fibrogenesis.[6] It is now clear that TGF-β evoked diverse cellular responses by binding to and activating specific cell-surface receptors that have intrinsic serine/threonine kinase activity. The activated TGF-β

receptors stimulate the phosphorylation of receptor-regulated Smad2 and Smad3 proteins (R-smads), which in turn form complexes with Smad4. This complex translocates from cytoplasm into nucleus, where the Smads regulate the transcription of target genes, including Smad7.[7,8] Smad7 is an inhibitory Smad that negatively regulates Smad2 and Smad3 activation and functions by targeting the TGF-β1 receptor and Smads for degradation via the ubiquitin proteasome degradation mechanisms.[9–11] It has been found that the disruption of *Smad7* gene promotes renal fibrosis in mouse models of UUO and ANG II-induced hypertension,[12,13] but, overexpression of Smad7 inhibits both renal fibrosis in rat model of unilateral ureteral obstruction (UUO) and EMT by blocking Smad2 activation in renal tubular epithelial cells.[14,15] However, it is also known that TGF-β1 is an anti-inflammatory cytokine, thus therapies with general blockade of TGF-β1 may risk in enhancing inflammatory response, which largely limited the development of anti-TGF-β therapy clinically. Thus, understanding deeply the mechanisms of TGF-β/Smad signaling in diseases associated with fibrosis and developing agents that antagonize TGF-β post-receptor signaling are critical for nephropathology research.[16,17]

Astragaloside IV (AS-IV) is a pure saponin isolated from *Astragalus membranaceus* (*Fisch*) *Bge*. Many studies have reported that AS-IV possesses a variety of pharmacological actions, such as anti-hypertension, positive inotropic action, anti-inflammation,[18] and anti-myocardial injury.[19] In particular, AS-IV has been considered as a renal protective agent. A number of studies demonstrated that AS-IV could inhibit kidney injury via anti-inflammation, inhibiting oxidative stress, and NF-κB-mediated inflammatory genes expression,[20–22] attenuate podocyte injury via regulation of MAPK pathway,[23] and ameliorate potocyte apoptosis by attenuating ROS production.[24] Recent report showed that AS-IV has an inhibitory action on EMT *in vitro*,[25] and AS-IV synergized with ferulic acid has a dramatic efficacy in inhibiting renal tubulointerstitial fibrosis *in vivo* and *in vitro*.[26] However, the role and mechanisms by which AS-IV inhibits renal fibrosis remain largely unknown until now. Therefore, in the present study, we investigated the *in vivo* and *in vitro* efficacy of AS-IV on UUO-induced and TGF-β-induced expression of pro-fibrotic genes and proteins, deposition of ECM proteins, and TGF-β/Smad signaling. Our findings provide the clear evidence that AS-IV has the potential to be developed as a therapeutic agent to prevent renal fibrosis.

Materials and methods

Materials

Antibodies including anti-TGF-β1, anti-connective tissue growth factor (anti-CTGF), anti-collagen I, anti-collagen III, and anti-Smad7 were purchased from Santa Cruz Biotechnology (Santa Cruz, CA). Anti-fibronectin, anti-phosphorylated Smad2, anti-Smad2, anti-phosphorylated Smad3, anti-Smad3, anti-GAPDH, and horseradish peroxidase (HRP)-labeled goat anti-rabbit or -mouse IgG were purchased from Cell Signaling Technology (Danvers, MA). Anti-α-SMA was purchased from Sigma-Aldrich (St. Louis, MO, USA). Recombinant TGF-β1 was purchased from Peprotech (Hamburg, Germany). Primers were synthesized from Sangon (Shanghai Co. Ltd., China). AS-IV was purchased from the National Institutes for Food and Drug Control, Shanghai, China, and purity was 98% with determination of high performance liquid chromatography (HPLC) analysis. The compound was prepared as a suspension in the medium of 0.5% carboxymethyl cellulose (CMC) for animal study and was dissolved in 1% dimethyl sulfoxide (DMSO; Sigma-Aldrich) at a concentration of 100 μmol/L as a stock solution for the cellular experiments.

Animal and experimental protocol

Male Sprague-Dawley rats (200–250 g) were obtained from Shanghai Slac Laboratory Animal Co., Ltd. (Shanghai, China). All experimental procedures were conducted in accordance with the National Institutes of Health Guide for the Care and Use of Laboratory Animals and were approved by the ethics committee of Putuo Hospital, Shanghai University of Traditional Chinese Medicine. The animals were given free access to water and fed a standard rat chow and were housed in an air-conditioned room at 25°C under 12 h light–dark cycles. Ninety rats were divided randomly into six groups ($n = 15$ for each group): (1) sham group, (2) UUO group, (3) UUO + enalapril group ($4\,mg{\cdot}kg^{-1}{\cdot}d^{-1}$, diluted in 0.5% CMC) as a positive control, and (4) UUO + AS-IV groups at doses of 3.33, 10, and 33 $mg{\cdot}kg^{-1}{\cdot}d^{-1}$ (diluted in 0.5% CMC). For UUO groups, rats were anesthetized with sodium pentobarbital ($50\,mg{\cdot}kg^{-1}$ intraperitoneally), then a midline incision of the abdomen was made, and the left ureter was ligated with 4-0 silk at three points and cut between the distal ligatures. The sham-operated rats underwent a similar procedure, but without ureteral ligation. The test compounds were given to rats by oral gavage daily for 14-day period on the day of the operation. At 14 days after UUO, the animals were sacrificed and the left kidneys were carefully removed and sagittally sliced into two parts. The first part was snap frozen in liquid nitrogen and kept at −80°C for protein and RNA extraction, and second part was immersed into 10% neutral-buffered formalin for histopathological and immunohistochemical examinations.

Renal function test

At 14 days after UUO operation, rat serum was collected from the abdominal aorta blood after centrifugation to detect serum creatinine (Scr) and blood urea nitrogen (BUN), which were used to estimate renal function. Scr and BUN were determined by the creatinine colorimetric assay kit (BioVision, USA) and BUN colorimetric detection kit (Arbor, USA) following the manufacturer's protocol, respectively.

Cell culture and treatment

The NRK-49F cells (rat renal fibroblasts) obtained from American Type Culture Collection (ATCC, Manassas, VA) were used between passages 4 and 18. They were cultured in complete RPMI 1640 (Gibco, USA) supplemented with 10% heat-inactivated fetal bovine serum (FBS, Gibco, USA),

100 U·mL^{-1} penicillin and 100 mg·mL^{-1} streptomycin in an atmosphere of 5% carbon dioxide and 95% air at 37°C. The NRK-49F cells were trypsinized using 0.25% trypsin-EDTA (Sigma-Aldrich) and seeded on six-well plates with complete medium that contained 10% FBS till subconfluence. In order to determine the optimal dose of TGF-β1 to stimulate α-SMA and fibronectin expression, first, the NRK-49F cells were treated with TGF-β1 at dosages of 0, 0.1. 0.5. 1.0, 2.0, and 5.0 ng·mL^{-1} and at various times of 0, 2, 4, 6, 12, and 24 h. Next, 3-(4, 5-dimethylthiazol-2-yl)-2, 5-diphenyl tetrazolium bromide (MTT) assay and lactate dehydrogenase (LDH) assay were performed to evaluate cytotoxicity to the NRK-49F cells. Briefly, cells were cultured at a density of 4×10^4 cells·mL^{-1} in 100 μL 1640 containing 1.0% FBS in 96-well microplates. Then AS-IV at dosages of 0, 5, 10, 20, 30, 40, 60, 80, and 100 μmol/L was added individually to the medium. In control cultures, the cells were exposed to equal amount of DMSO at the same cell density. After 24 h of incubation, the supernatants were collected and centrifuged at 250 *g* for 10 min, and the extents of cytotoxicity of AS-IV were measured by MTT assay kit (Sigma-Aldrich) and LDH release kit (BioVision) using a microplate reader (Bio-Rad Laboratories, CA). All measurements were performed in duplicate. Eventually, to evaluate the inhibitory effect of AS-IV on TGF-β1-induced profibrogenic responses, the NRK-49F cells were pre-treated with AS-IV at dosages of 0, 2, 5, 10, 20, and 40 μmol/L for 30 min, TGF-β1 was then added. After treatment with AS-IV for 6 h, the NRK-49F cells were harvested to determine RNA levels and after treatment with AS-IV for 24 h, protein expression was measured.

Histology and immunohistochemistry

For histological analysis, renal tissues fixed with 10% neutral-buffered formalin were embedded in paraffin. Paraffin sections (3 μm thick) were stained with hematoxylin-eosin, and tubulointerstitial injury was according to the published criteria.[27] In order to further analyze the degree of interstitial collagen deposition, Masson's-modified trichrome-staining sections were graded.[28]

For immunohistochemistry analysis, paraffin-embedded sections were deparaffinized, washed with phosphate-buffered saline (PBS), and treated with 3% H_2O_2 for 5 min. An antigen retrieval protocol in which sections were heated in 10 mmol/L citrate buffer (pH 6.0) for 10 min. Sections were then incubated with antibodies for anti-CTGF (1:50 dilution), anti-α-SMA (1:500 dilution), anti-collagen 1 (1:50 dilution), anti-collagen 3 (1:50 dilution), anti-fibronectin (1:1000 dilution), anti-phosphorylated-Smad2 (1:250 dilution), and anti-phosphorylated-Smad3 (1:250 dilution) at 4°C overnight. After washing, sections were incubated with appropriate biotin-conjugated goat anti-rabbit or-mouse IgG antibodies, and then treated with reagents from a Vecta-Elite streptavidin-peroxidase kit (Vector Laboratories, Burlingame, CA) with a benzidine substrate for color development. The stained sections were developed with diaminobenzidine to produce brown products and counterstained with hematoxylin.

Western blot analysis

Renal tissues or cultured NRK-49F cells were lysed in a buffer (50 mmol/L Tris at pH of 7.5, 1 mmol/L EDTA, 150 mmol/L NaCl, 20 mmol/L NaF, 0.5% NP-40, 10% glycerol, 1% protease inhibitor cocktail and 1% phosphatase inhibitor cocktail) by sonication on ice. The lysates were cleared by centrifugation at 13,000 *g* at 4°C for 20 min and the supernatant was collected. Then the protein concentration was determined by bicinchoninic acid (BCA) protein assay kit (Pierce, Rockford, IL).

Equal amounts of protein (40 μg) were separated by 10% SDS polyacrylamide gel electrophoresis and transferred to PVDF (Millipore, USA) membrane. Following blocked with 5% bovine serum albumin (BSA) in TBS-Tween-20 for 2 h, the membrane was incubated with primary antibodies individually with anti-TGF-β1 (1:1000 dilution), anti-CTGF (1:500 dilution), anti-α-SMA (1:1000 dilution), anti-collagen 1 (1:200 dilution), anti-collagen 3 (1:200 dilution), anti-fibronectin (1:10,000 dilution), anti-phosphorylated-Smad2 (1:1000 dilution), anti-Smad2 (1:1000 dilution), anti-phosphorylated-Smad3 (1:1000 dilution), anti-Smad3 (1:1000 dilution), anti-Smad7 (1:200 dilution), and anti-glyceraldehyde-3-phosphate dehydrogenase (GAPDH, 1:1000 dilution) at 4°C overnight. After three washes in TBS-Tween-20, the membranes were incubated with HRP-labeled goat anti-rabbit or -mouse IgG for 1 h at room temperature. Protein bands were visualized using enhanced ECL (Millipore) and X-ray film. The ratio of the protein interested was subjected to GAPDH and was densitometrically analyzed by Multi-Analyst software program (Version 1.01; Bio-Rad).

Quantitative real-time PCR

Total RNA was extracted from frozen renal samples or cultured cells using the RNeasy Mini Kit (QIAGEN, Valencia, CA) following the manufacturer's protocol. Briefly, 1 μg of total RNA was reverse transcribed using the AMV First Strand cDNA Synthesis kit (QIAGEN) and synthesized complementary DNA was amplified by a standard PCR protocol using SYBR green PCR master mix (QIAGEN). Primers were synthesized from Sangon Biotech Co. Ltd. (Shanghai, China). The sequences of rat-specific primers for TGF-β1, CTGF, α-SMA, fibronectin, collagen I, collagen III, Smad7, and GAPDH used in the study were enlisted in Table 1. Cycling conditions were: 15 min preincubation at 95°C, 10 s denaturation at 95°C, 31 s annealing at 58°C for 40 cycles using ABI PRISM 7300 sequence detection system (Applied Biosystems). Each reaction was amplified in triplicate and the threshold cycles (Ct) were calculated using the ΔΔCt method. Relative gene expression was normalized with GAPDH as an internal reference.

RNA interference and plasmid transfection

The Smad7-specific siRNA were synthesized and purchased from GenePharma (Shanghai Co. Ltd.). An adopted non-silencing scrambled siRNA that was not complementary to any rat gene was used as control. For siRNA transfection, cells were plated in six-well culture plates at density of 4×10^5 and transfected with siRNA by using

Table 1 Primers used for quantitative real-time PCR

Genes	Forward primer	Reverse primer
TGF-β1	5′-GTCAACTGTGGAGCAACACG-3′	5′-GTCTCCTTGGTTCAGCCACT-3′
CTGF	5′-CGAGCTAAATTCTGTGGAGT-3′	5′-CCGGTAGGTCTTCACACTGGT-3′
α-SMA	5′-TTCGTGACTACTGCTGAGCG-3′	5′-AAGCGTTCATTCCCGATGGT-3′
Fibronectin	5′-TTATGACGACGGGAAGACCT-3′	5′-GCTGGATGGAAAGATTACTC-3′
Collagen I	5′-TGGTGAGACGTGGAAACCTG-3′	5′-CTTTGCATAGCACGCCATCG-3′
Collagen III	5′-CTGGACCAAAAGGTGATGCTG-3′	5′-TGCCAGGGAATCCTCGATGTC-3′
Smad7	5′-GCTGGTACAGAAAGTGAGGAG-3′	5′-GTCCGGGTTGTCCAGTGTG-3′
GAPDH	5′-TGCACCACCAACTGCTTAGC-3′	5′-GGCATGGACTGTGGTCATGAG-3′

Lipofectamine 2000 (Invitrogen, Calsbad, CA) according to the manufacturer's instructions. After 48 h transfection, cells were harvested for protein analysis using Western blot.

Statistical analyses

Statistical analysis was performed using GraphPad Prism software version 5.0 (GraphPad Prism software Inc., San Diego, CA). Results were presented as mean ± standard error of mean (SEM). The differences among multiple groups were evaluated by a one-way analysis of variances (ANOVA). The differences between two groups were determined by *t* test. Probability (*P*) value of less than 0.05 was considered to indicate statistical significance.

Results

Effect of AS-IV on renal histology and renal function in rat UUO model

As shown in Figure 1A, the paraffin-embedded sections stained with H&E exhibited significant tubulointerstitial damage, including tubular atrophy, inflammatory cells infiltration, and interstitial fibrosis in UUO kidneys compared with those in sham-operative kidneys (sham group). In contrast, tubulointerstitial damage and inflammatory response were reduced in dose-dependent manner ($P < 0.01$ or 0.001) in UUO kidneys taken from AS-IV-treated rats compared with vehicle-treated UUO kidneys, which were demonstrated by semiquantitative histomorphometry analysis (Figure 1B). UUO also induced an increase of collagen on the Masson's trichrome-stained kidney sections compared with sham-operative kidneys (Figure 1C). However, treatment with AS-IV in UUO kidneys led to less collagen deposition compared with vehicle-treated UUO kidneys. This was also confirmed by semiquantitative assessment of the fibrotic area on the Masson's trichrome-stained kidney sections (Figure 1D). Determination of functional changes showed that serum creatinine (Scr) and blood urea nitrogen (BUN) levels significantly enhanced in UUO animals compared with sham-operative animals, and attenuated in UUO animals treated with AS-IV (Figure 2A, B). The similar improvements on pathological and functional injuries were obtained by UUO animals treated with enalapril.

Effect of AS-IV on expression of pro-fibrotic and α-SMA genes in rat UUO model

UUO-induced tubulointerstitial fibrosis is due to activation of resident renal tubular cells and interstiblasts that were elicited by pro-fibrotic protein expression and accumulation of ECM pomponents. As shown in Figures 4 and 5, UUO increased the major pro-fibrotic factors TGF-β1 and CTGF levels compared with those in sham-operative kidneys, but prevented by treatment with AS-IV determined by RT-PCR and Western blot. Immunohistochemistry analysis further revealed that the expression level of CTGF was significantly increased in the UUO kidneys compared with sham-operative kidneys ($P < 0.001$) and was decreased after treatment with AS-IV and enalapril compared with the vehicle-treated UUO kidneys ($P < 0.01$, Figure 3B). Furthermore, α-smooth muscle actin (α-SMA), a marker of myofibroblasts, was barely detectable in sham-operated kidneys (Figure 3C, D). UUO led to the significant up-regulation of α-SMA expression in the obstructed kidneys, as shown by Western blot, RT-PCR, and immunostaining. In contrast, treatment with AS-IV could attenuate α-SMA expression in dose-dependent manner. The similar results were obtained from UUO animals treated with enalapril. As above mentioned, AS-IV could reduce the gene up-streams of ECM and modulates ECM accumulation. Thus, we next determined the effects of AS-IV treatment on accumulation of ECM proteins in UUO kidneys. The induction of UUO in rats led to the accumulation of fibronectin, collagen I and III shown by Western blot, RT-PCR, and immunostaining. Treatment with AS-IV or enalapril in UUO induced the obstructed kidneys and diminished the augmented expression of ECM proteins (Figures 3–5).

Effect of AS-IV on TGF-β1-induced profibrogenic factors and ECM accumulation in cultured NRK-49F cells

TGF-β1, as a potent fibrogenic cytokine inducer, has been reported to stimulate fibrogenesis in renal fibroblasts in the concentration range between 1.0 and 5 $ng \cdot mL^{-1}$.[2,26,29,30] As shown in Figure 6, in this study, we determined an appropriate dosage of TGF-β1 to stimulate fibrotic response in the NRK-49F cells. The results showed that TGF-β1 stimulation enhanced α-SMA and fibronectin mRNA and protein expression in the NRK-49F cells in a time- and concentration-dependent manner with an appropriate dosage of

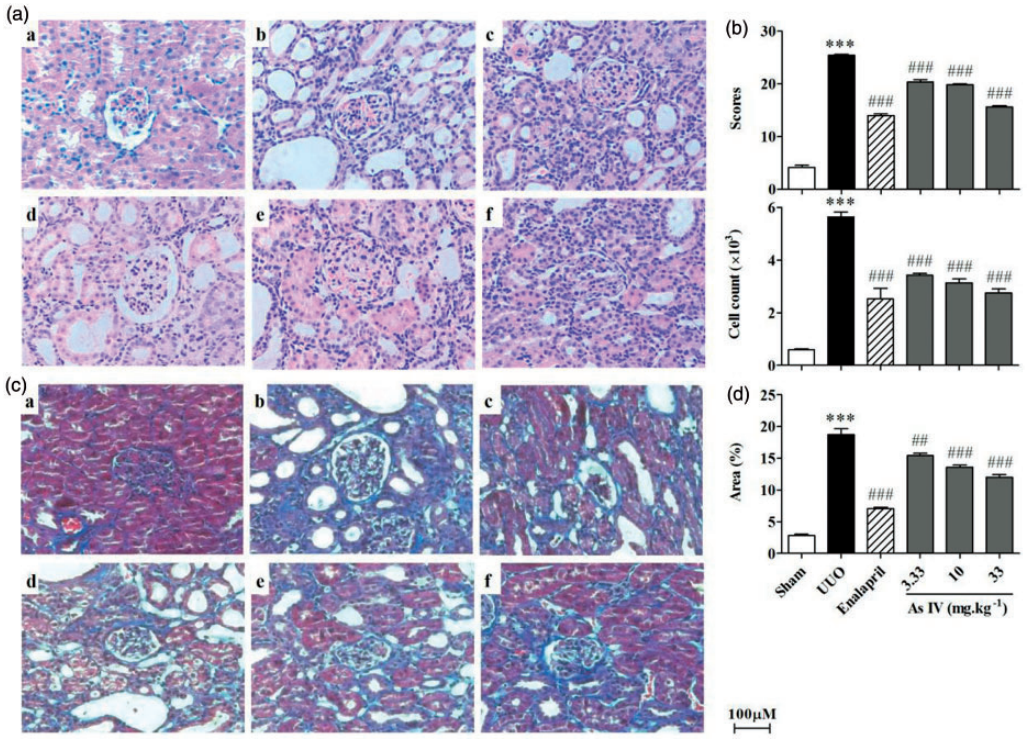

Figure 1 AS-IV treatment attenuates renal damage in a dosage-dependent manner in UUO kidneys. (A) Representative hematoxylin–eosin (HE)-stained kidney sections from Sham (a), UUO (b), enalapril (c), AS-IV 3.33, 10, and 33 mg·kg^{-1} (d–f) groups. (B) Histopathological scores and inflammatory cells count within the tubulointerstitium from sections similar to those shown in (A). (C) Representative Masson's modified trichrome stained kidney sections from sham (a), UUO (b), enalapril (c), AS-IV 3.33, 10, and 33 mg·kg^{-1} (d–f) groups. (D) Quantitative analysis of the extent of renal interstitial expansion (area %) from sections similar to those shown in. Data represent mean ± SEM for at least 10 independent experiments. $^{***}P < 0.001$, compared with sham group; $^{\#\#}P < 0.01$, $^{\#\#\#}P < 0.001$ compared with UUO group. Magnification: × 200

TGF-β1 at 1.0 ng·mL^{-1}. To clarify cytotoxicity of AS-IV on the NRK-49F cells for *in vitro* experiment, MTT and LDH arrays were performed (Figure 7A, B). We found that AS-IV at concentration range among 2, 5, 10, 20, and 40 μmol/L does not influence the viability of cultured fibroblasts. Thus, AS-IV at and below 40 μmol/L does not exert its action by inhibiting cell growth or by inducing cell death. Subsequently, we determined the inhibitory effect of AS-IV on TGF-β1-induced overexpression of α-SMA, CTGF, and ECM proteins in the NRK-49F cells. The expression level of α-SMA was increased by TGF-β1 stimulation of the NRK-49F cells. This increase in expression of α-SMA protein was attenuated by AS-IV, dose-dependently. The activation of resident renal tubular cells and interstiblasts was considered as the main source of ECM proteins. We therefore observed whether AS-IV could suppress TGF-β1 induced expression of ECM proteins in the NRK-49F cells. As shown in Figure 7C–J, fibronectin, collagen I and III proteins, which are the major ECM components in interstitial fibrosis, were enhanced to 1.9 ± 0.1, 2.2 ± 0.2, and 2.5 ± 0.4 fold compared with control level in the NRK-49F cells. Treated cells with AS-IV could concentration-dependently inhibit this up-regulation of ECM protein. The further experiment was carried out to elucidate the influence of AS-IV on upstreams of ECM such as CTGF, a profibrogenic factor, in cells stimulated by TGF-β1. The results showed that TGF-β1 increased the expression of CFGF proteins by 3.4 ± 0.3

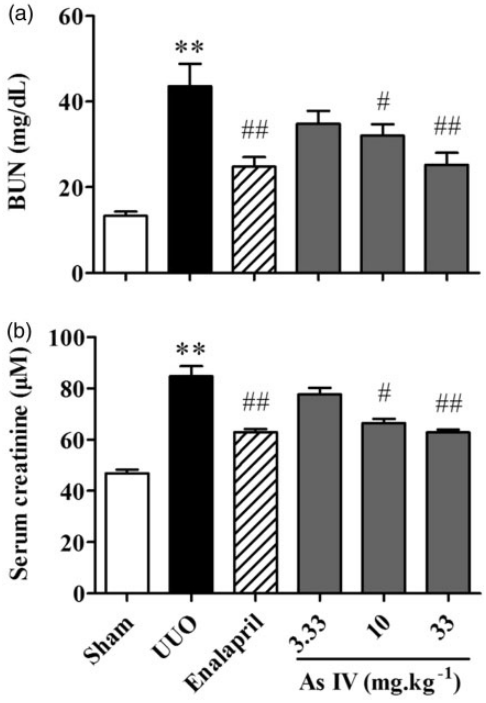

Figure 2 AS-IV treatment improves renal function in a dosage-dependent manner in UUO kidneys. BUN (A) and serum creatinine (B) in the Sham, UUO, enalapril, AS-IV (3.33, 10 and 33 mg·kg^{-1}) groups. Data represent mean ± SEM for at least 10 independent experiments. $^{**}P < 0.01$, compared with the sham group; $^{\#}P < 0.05$, $^{\#\#}P < 0.01$ compared with the UUO group

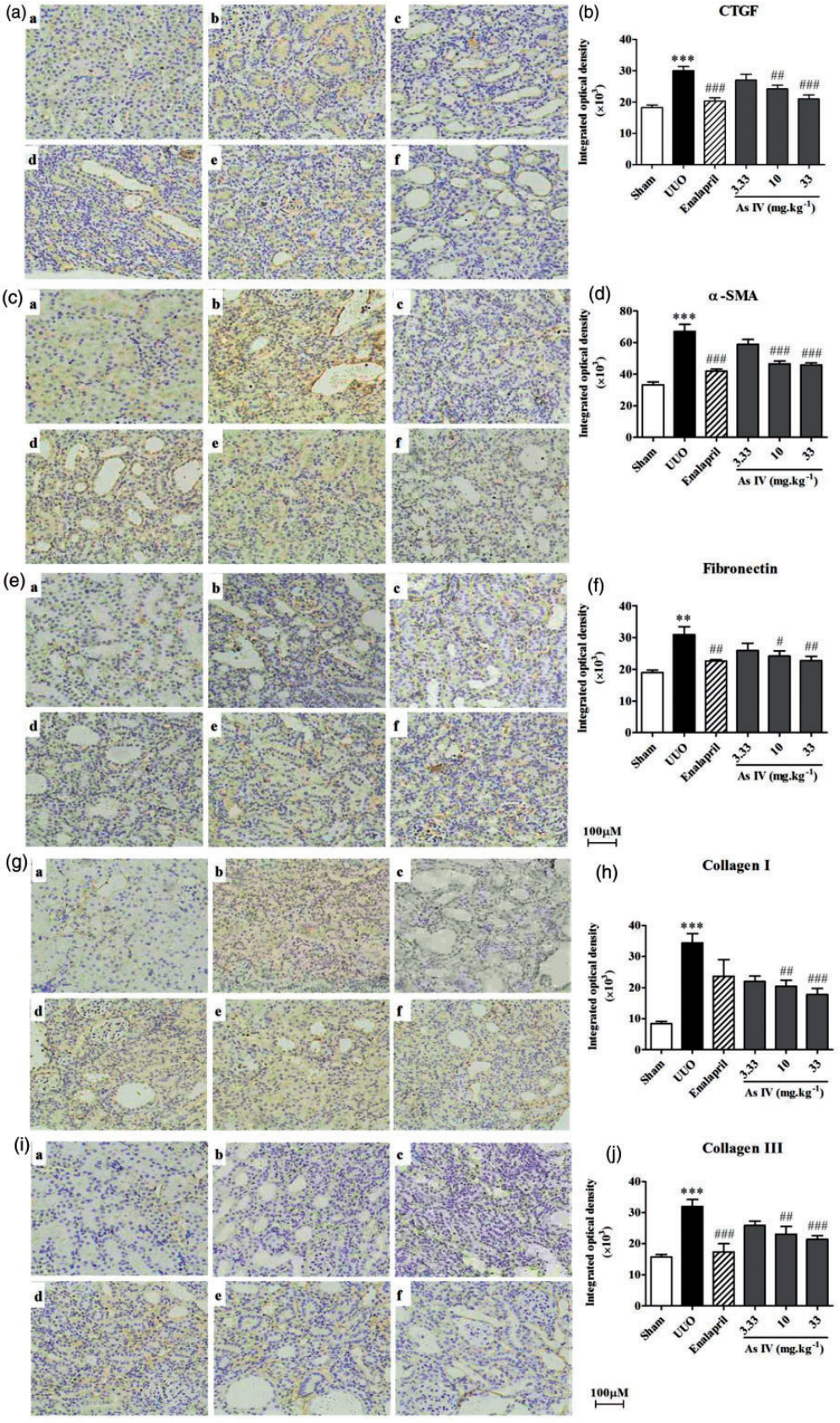

Figure 3 Treatment with AS-IV decreases CTGF, α-SMA, fibronectin, collagen I and III expression by immunohistochemistry in UUO kidneys. (A, C, E, G, I) Representative photomicrographs of CTGF, α-SMA, fibronectin, collagen I and III immunohistochemistry on kidney sections from the Sham (a), UUO (b), enalapril (c), AS-IV 3.33, 10, and 33 mg·kg^{-1} (d–f) groups. (B, D, F, H, J) Quantitative analysis of CTGF, α-SMA, fibronectin, collagen I and III expression from sections similar to those shown in A, C, E, G, I. Data represent mean ± SEM for at least 10 independent experiments. $^{**}P < 0.01$, $^{***}P < 0.001$, compared with the sham group; $^{\#}P < 0.05$, $^{\#\#}P < 0.01$, $^{\#\#\#}P < 0.001$ compared with the UUO group. Magnification: ×200

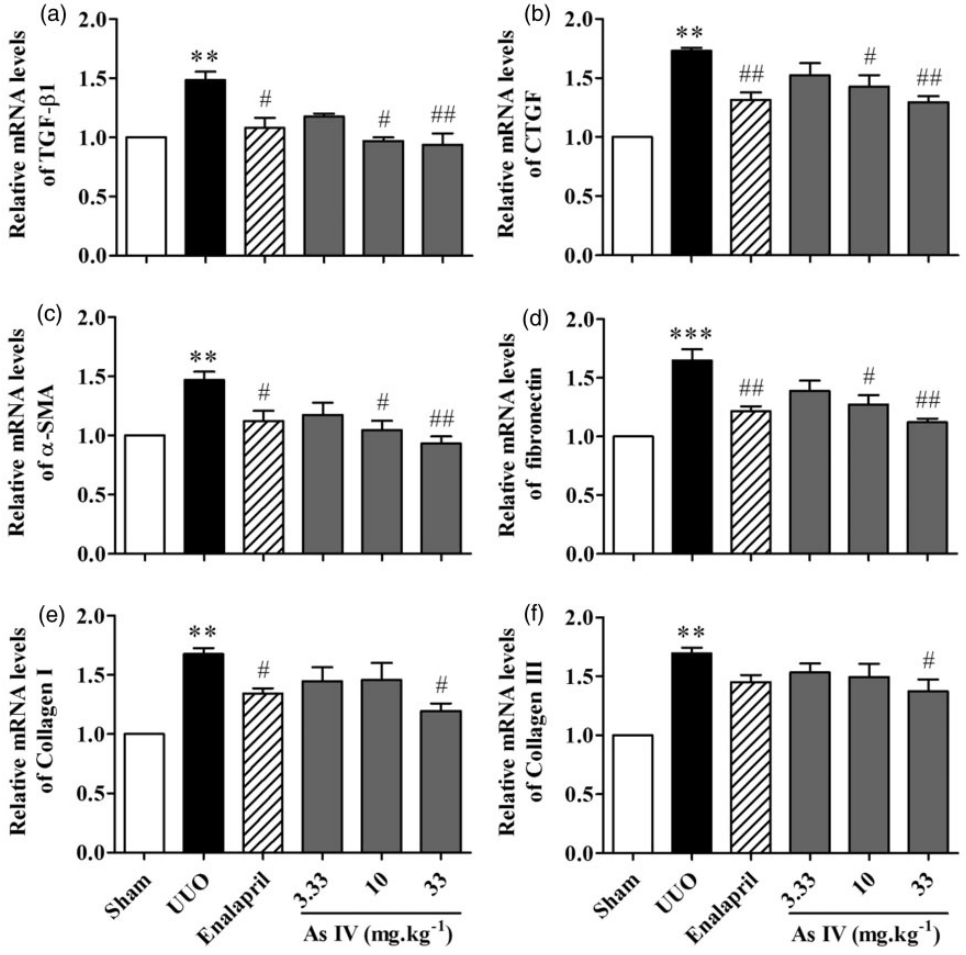

Figure 4 Treatment with AS-IV decreases TGF-β1, CTGF, α-SMA, fibronectin, collagen I and III gene expression in UUO kidneys. (A–F) Real-time PCR shows the relative mRNA levels of TGF-β1, CTGF, α-SMA, fibronectin, collagen I and III expression in kidneys. Data represent mean ± SEM for at least three independent experiments. $^{**}P < 0.01$, $^{***}P < 0.001$, compared with the sham group; $^{\#}P < 0.05$, $^{\#\#}P < 0.01$ compared with the UUO group

fold, and treatment with AS-IV reduced this CTGF expression in concentration-dependent manner in the NRK-49F cells, suggesting that a possible mechanism underlying attenuation of ECM accumulation.

Blockade of Smad2/3 activation by up-regulation of Smad7 is a key mechanism by which AS-IV prevents renal fibrosis *in vivo* and *in vitro*

TGF-β-mediated fibrosis is positively regulated by P-Smad2/3 but negatively regulated by Smad7, thus we studied the mechanisms by which AS-IV represses profibrotic genes and ECM protein expression in UUO kidneys by determining TGF-β-mediated Smad signaling pathway. Immunohistochemistry analysis indicated that UUO induced the nuclear translocation of P-Smad2/P-Smad3, which was inhibited by AS-IV in dose-dependent fashion (Figure 8). Consistent with this observation, Western blot analysis showed that UUO induced the up-regulation of Smad2/Smad3 phosphorylation level but not 'total' Smad2/Samd3. By contrast, treatment with AS-IV in UUO kidneys led to the decrease of Smad2/Smad3 phosphorylation level in dose-dependent fashion (Figure 9). Recent studies have demonstrated that the disruption of *Smad7* gene could induce up-regulation of Smad2/Smad3 phosphorylation level, and overexpression of Smad7 could overcome Smad2/Smad3 phosphorylation in obstructive nephropathy.[12,14] In the present study, we found that UUO induced a down-regulation of Smad7 protein expression, and which was restored by treatment of AS-IV in UUO kidneys in dose-dependent fashion, suggesting that blockade of TGF-β/Smad signaling by enhancing the expression level of Smad7 is a possible mechanism for inhibition of UUO-induced renal fibrosis by AS-IV.

The mechanism of blockade of TGF-β/Smad signaling by up-regulation of Smad7 to prevent UUO-induced renal fibrosis was further carried out in the NRK-49F cells. The results obtained from Western blot analysis showed that treatment of cells with AS-IV could inhibit TGF-β1-stimulated Smad2 or Smad3 phosphorylation level but increased Smad7 expression in a concentration-dependent manner (Figure 10), and also attenuate TGF-β1-induced CTGF, α-SMA, fibronectin, and collagen I and III expression (Figure 11). The above results indicate that the inhibitory effect of AS-IV on TGF-β/Smad-mediated renal fibrosis is

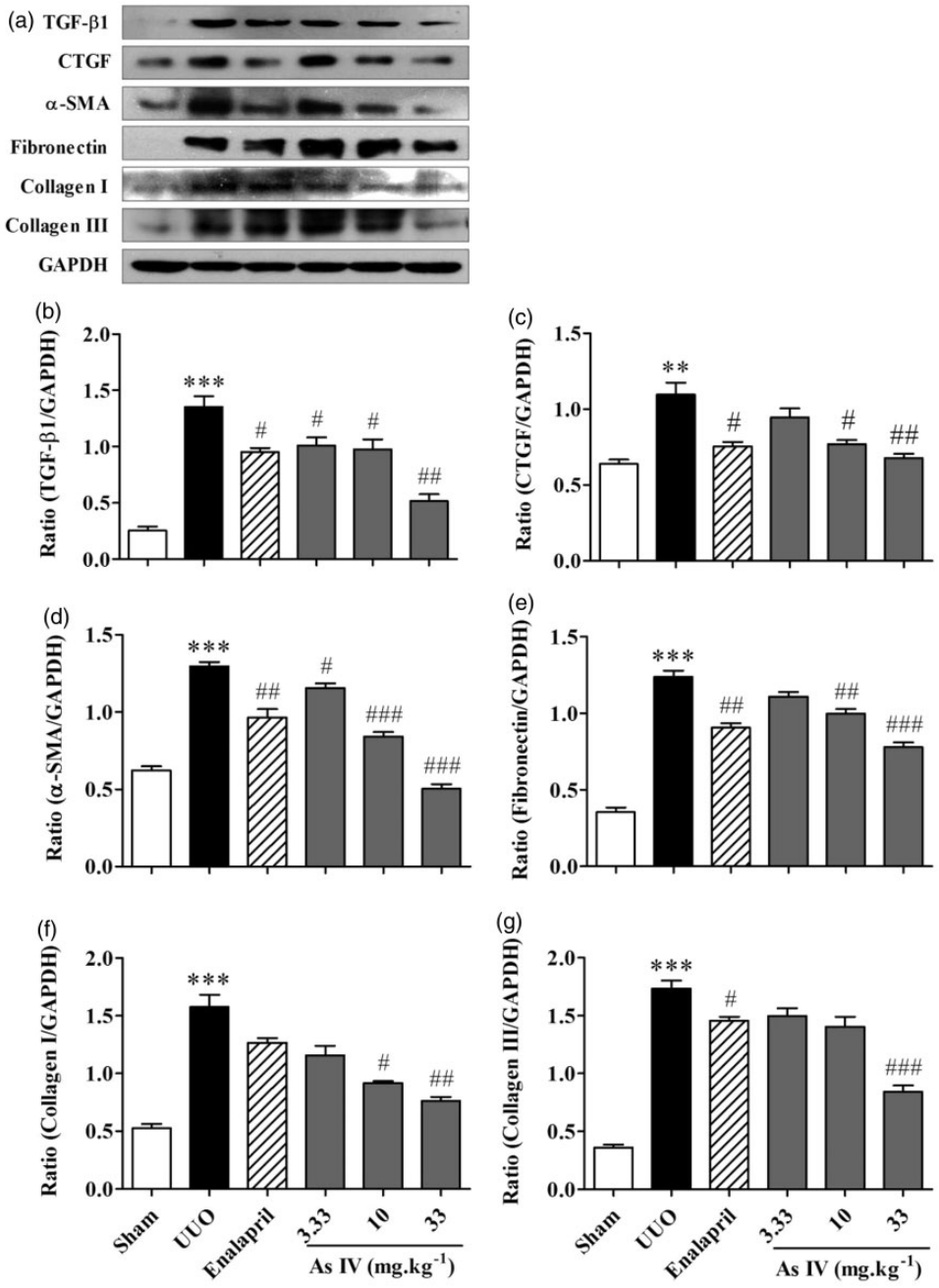

Figure 5 Treatment with AS-IV decreases TGF-β1, CTGF, α-SMA, fibronectin, collagen I and III protein expression in UUO kidneys. (A) Representative Western blot photographs showing levels of TGF-β1, CTGF, α-SMA, fibronectin, collagen I and III protein expressions in kidneys. (B–G) Quantitative analysis of the relative ratios of TGF-β1, CTGF, α-SMA, fibronectin, collagen I and III protein normalized with GAPDH. Data represent mean ± SEM for at least three independent experiments. $^{**}P < 0.01$, $^{***}P < 0.001$, compared with the sham group; $^{\#}P < 0.05$, $^{\#\#}P < 0.01$, $^{\#\#\#}P < 0.001$ compared with the UUO group

associated with overexpression of Smad7. In order to demonstrate this mechanism, *Smad7* gene was knocked down from the NRK-49F cells using siRNA technique. Western blot analysis shows that AS-IV does not exert its inhibitory action on TGF-β1-stimulated Smad2 or Smad3 phosphorylation, and CTGF, α-SMA, fibronectin, and collagen I and III expression after knockdown of Smad7 from the NRK-49F cells *in vitro*, suggesting that up-regulation of Smad7 is key mechanism for attenuation of renal fibrosis by treatment with AS-IV in the obstructed nephropathies.

Discussion

In the present study, we demonstrated that AS-IV dose-dependently inhibited UUO-induced renal fibrosis and function injury, which are associated with TGF-β-stimulated Smad 2/3 phosphorylation, profibrotic genes TGF-β1 and CTGT, myofibroblast marker α-SMA, and ECM accumulation in rat renal injury model. In addition, AS-IV also effectively inhibited TGF-β1-stimulated Smad 2/3 phosphorylation, profibrogenic genes, α-SMA, and ECM

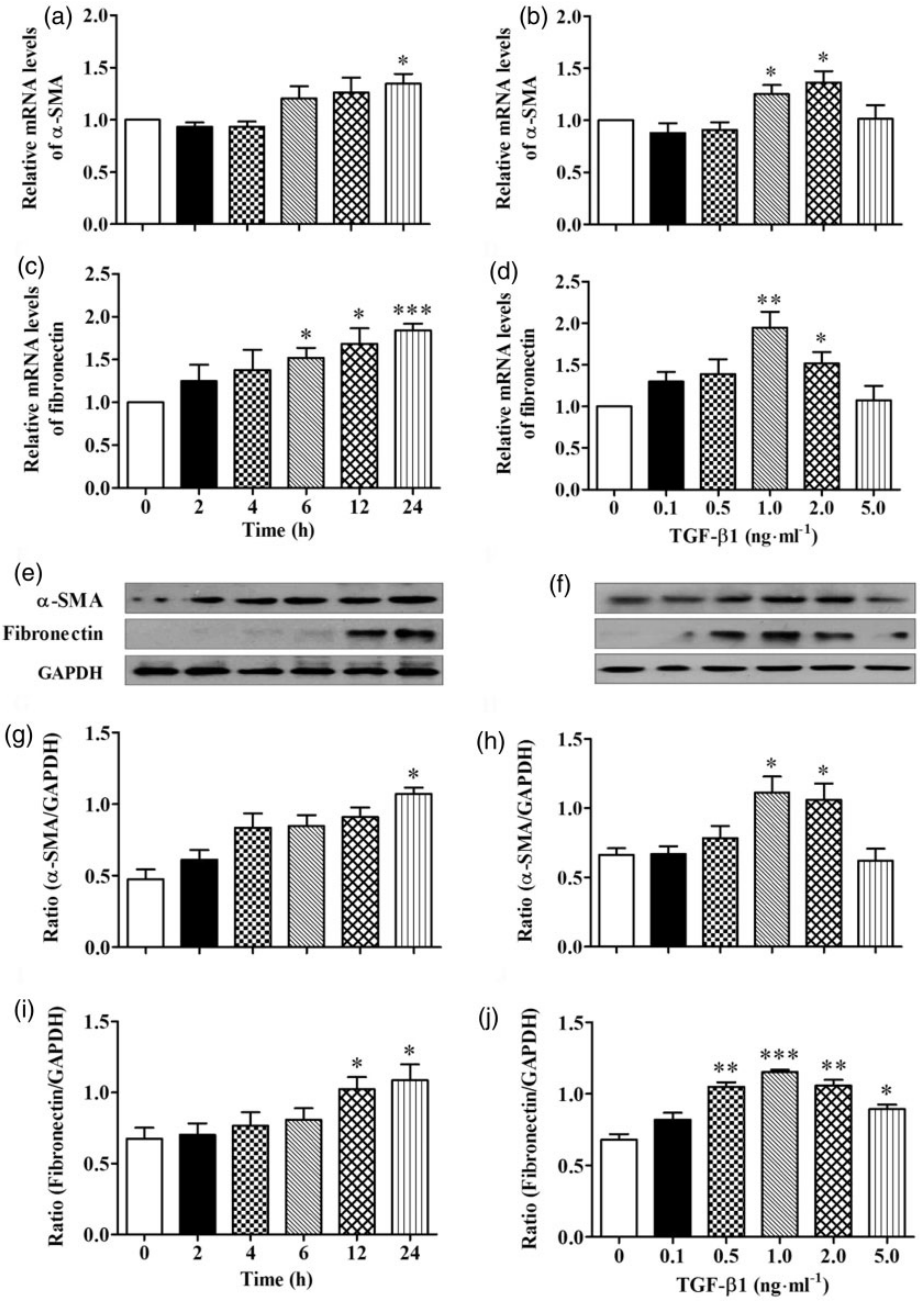

Figure 6 TGF-β1 induces α-SMA and fibronectin expression in a time- and dose-dependent manners in NRK-49 F cells. (A–D) Real-time PCR shows the time (TGF-β1 1 ng·mL^{-1}) and dose (24 h)-dependent effects of TGF-β1 on α-SMA and fibronectin mRNA expression in NRK-49F cells. (E–J) Western blot demonstrated that TGF-β1-treated cell exhibited α-SMA and fibronectin protein expression in a time- and dose-dependent manners. Data represent mean ± SEM for at least three independent experiments. *$P < 0.05$, **$P < 0.01$, ***$P < 0.001$, compared with the non-treated control

protein expression in a rat NRK-49F cell line. Furthermore, blockade of TGF-β/Smad signaling via induction of renal Smad7 could be the underlying mechanism by which AS-IV attenuated UUO-induced renal fibrosis *in vivo* and TGF-β1-stimualted profibrogenic factors and ECM production *in vitro*.

Evidences from the results obtained by this study, we consider that AS-IV inhibited TGF-β-induced renal pathological progressions in experimental tubulointerstitial fibrosis by multiple mechanisms. Pro-apoptotic effectors and/or profibrotic activation of tubular were initiated in response to TGF-β that led to tubular degeneration and atrophy. Moreover, induction of TGF-β1 may convert tubular epithelial cells and fibroblasts into activated myofibroblasts, which could be responsible for enhanced deposition of interstitial matrix by TGF-β/Smad signaling. The majority of activated fibroblasts called myofibroblasts in the damaged kidney could originate from tubular epithelium through the process of EMT.[31] α-SMA-positive myofibroblasts were identified as the primary cells type responsible

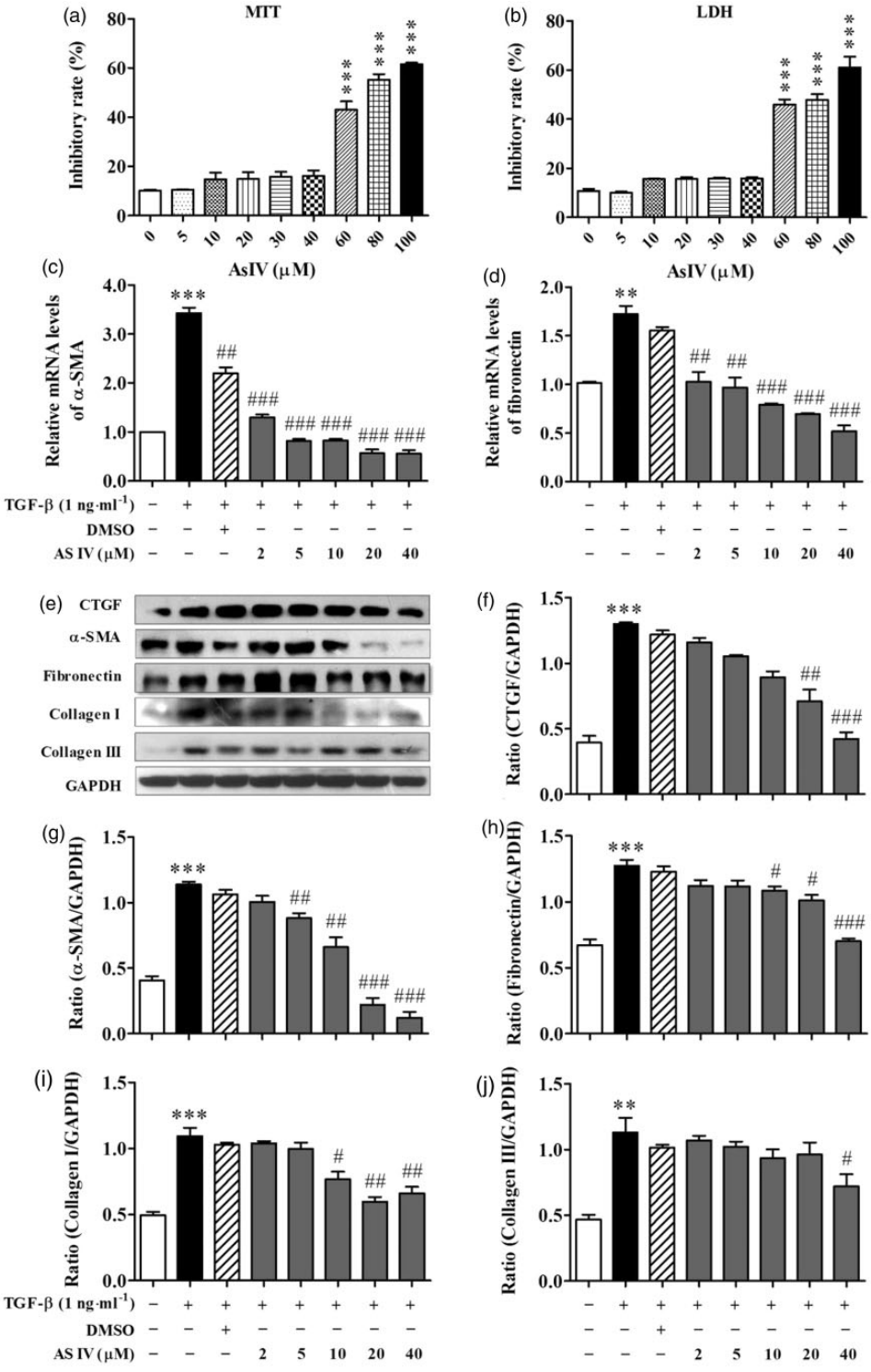

Figure 7 AS-IV decreases TGF-β-induced CTGF, α-SMA, fibronectin, collagen I and III expression dose-dependently in NRK-49F cells. (A, B) MTT and LDH release assays show the dose-dependent effects of AS-IV on cytotoxicity of NRK-49 F cells. (C, D) Real-time PCR shows the dose-dependent inhibitory effect of AS-IV on α-SMA and fibronectin mRNA expression. (E) Representative Western blot photographs showing levels of CTGF, α-SMA, fibronectin, collagen I and III protein expressions in TGF-β1 (1 ng·mL^{-1})-treated cells. (F–J) Summary histograms showing the ratio of CTGF, α-SMA, fibronectin, collagen I and III expressions relative to GAPDH from experiments similar to those shown in E. Data represent mean ± SEM for at least three independent experiments. $^{**}P < 0.01$, $^{***}P < 0.001$, compared with non-treated control; $^{\#}P < 0.05$, $^{\#\#}P < 0.01$, $^{\#\#\#}P < 0.001$ compared with TGF-β1 (1 ng·mL^{-1})-treated cells

for interstitial matrix accumulation and were considered specific for EMT in renal fibrotic diseases.[32] Moreover, in response to TGF-β1 resident fibroblasts can be activated, and tubular epithelial cells can transdifferentiate into myofibroblasts.[33,34] In the present study, the enhanced α-SMA expression in kidney of UUO rats and the TGF-β1-stimulaed α-SMA expression were significantly reduced by AS-IV. These observations indicated that TGF-β1 induced

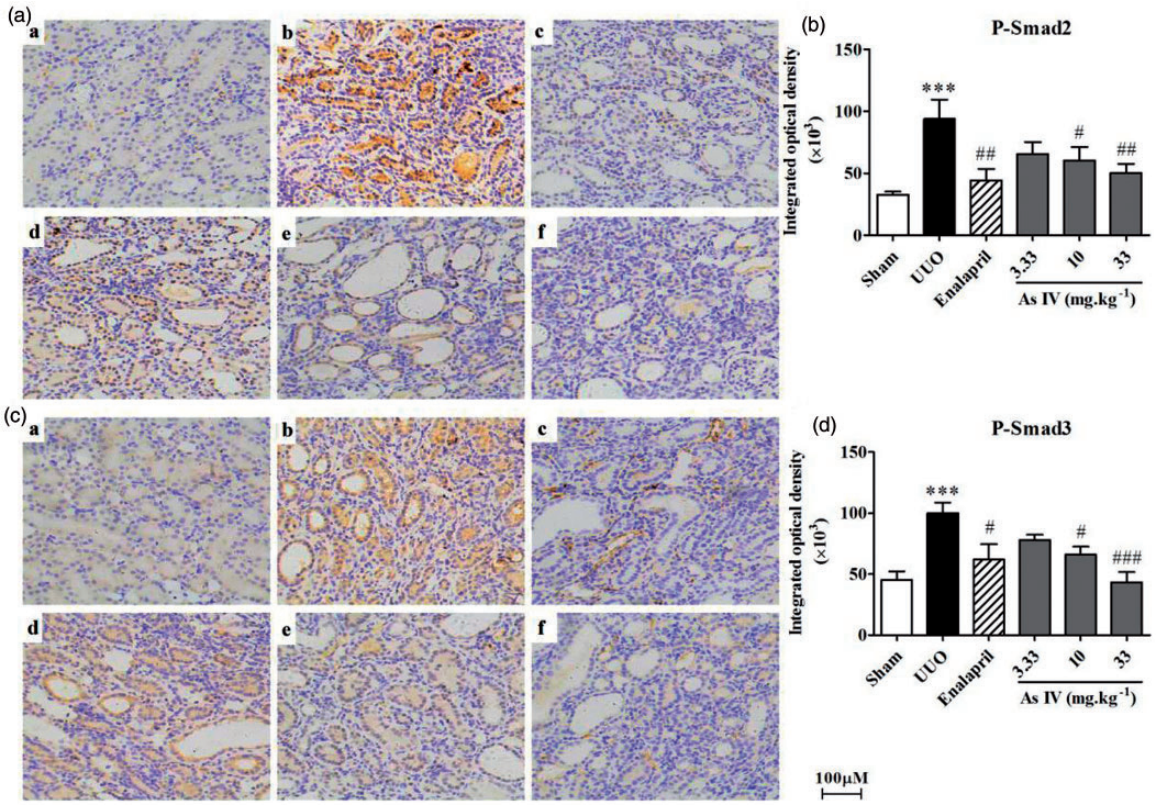

Figure 8 Treatment with AS-IV blocks activation of p-Smad2 and p-Smad3 in UUO kidneys. (A, C) Representative photomicrographs of p-Smad2 and p-Smad3 immunohistochemistry on kidney sections from the Sham (a), UUO (b), enalapril (c), AS-IV 3.33, 10 and 33 mg·kg^{-1} (d–f) groups. (B, D) Integrated optical density analysis of p-Smad2 and p-Smad3 expression from sections similar to those shown in (A, C). Data represent mean ± SEM for at least 10 independent experiments. $^{***}P < 0.001$, compared with the sham group; $^{\#}P < 0.05$, $^{\#\#}P < 0.01$, $^{\#\#\#}P < 0.001$ compared with the UUO group. Magnification: ×200

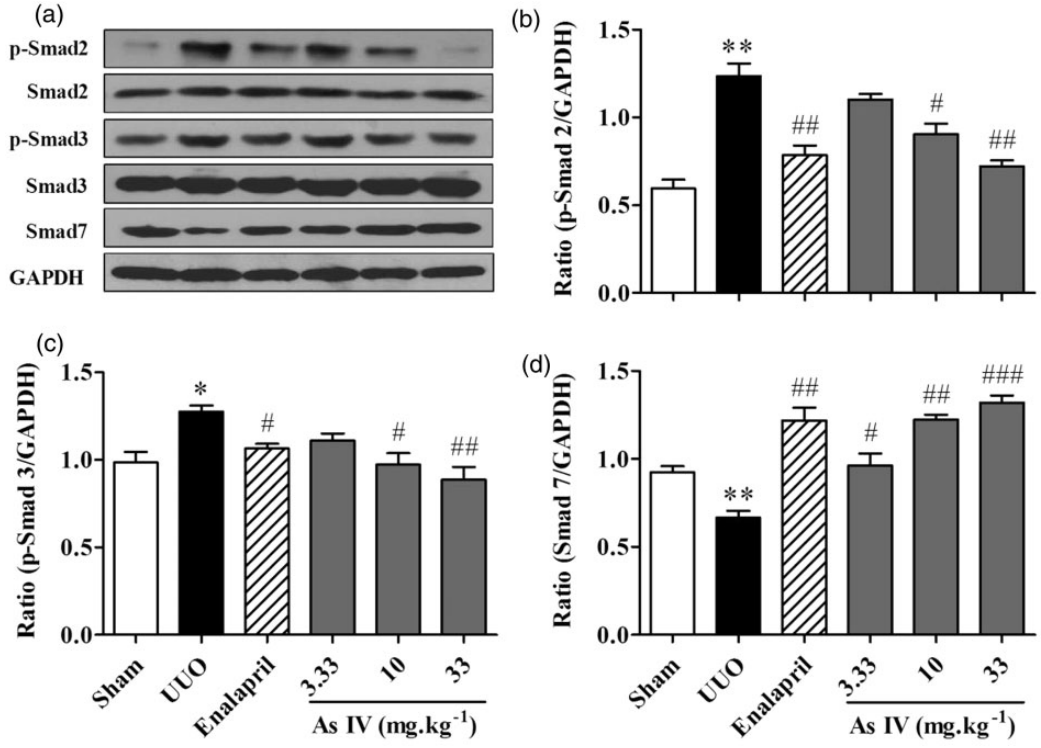

Figure 9 Treatment with AS-IV up-regulates Smad7, but decreases p-Smad2 and p-Smad3 expression in UUO kidneys. (A) Representative Western blot photograph showing expression levels of Smad2, p-Smad2, Smad3, p-Smad3, and Smad7 proteins in rat kidneys. (B–D) Quantitative analysis of the relative ratio of p-Smad2, p-Smad3, and Smad7 proteins normalized with GAPDH. Data represent mean ± SEM for at least three independent experiments. $^{*}P < 0.05$, $^{**}P < 0.01$, compared with the sham group; $^{\#}P < 0.05$, $^{\#\#}P < 0.01$, $^{\#\#\#}P < 0.001$ compared with the UUO group

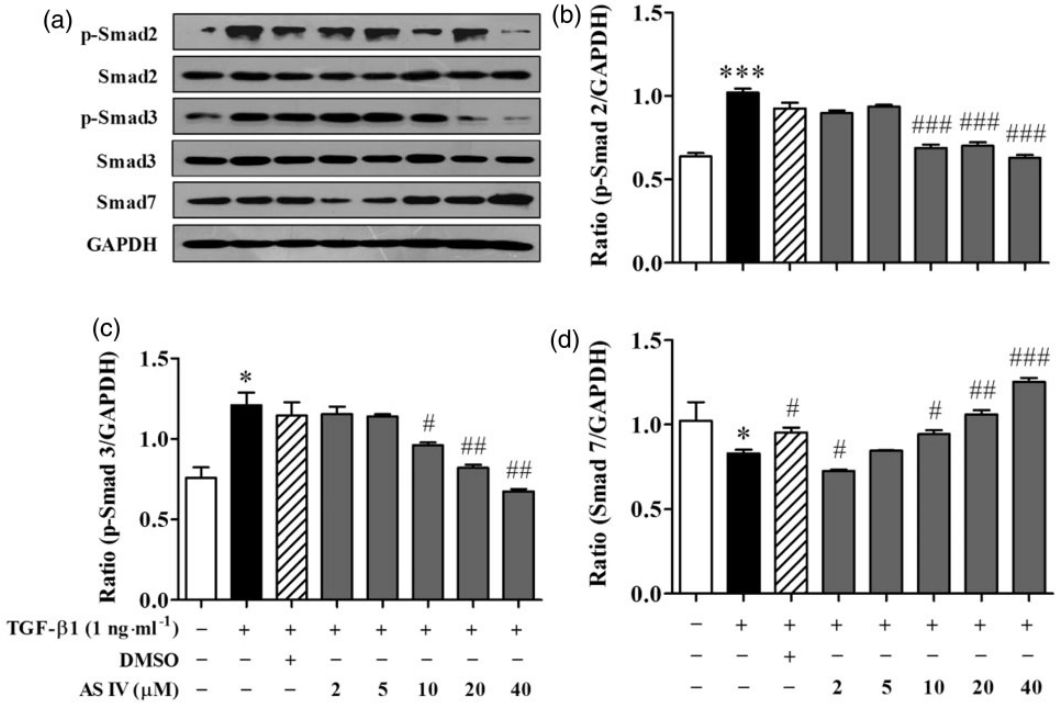

Figure 10 Treatment with AS-IV up-regulates Smad7, but decreases p-Smad2 and p-Smad3 expression in NRK-49 F cells. (A) Representative Western blot photograph showing expression levels of Smad2, p-Smad2, Smad3, p-Smad3, and Smad7 proteins in NRK-49 F cells. (B–D) Quantitative analysis of the relative ratio of p-Smad2, p-Smad3, and Smad7 proteins normalized with GAPDH. Data represent mean ± SEM for at least three independent experiments. $^{*}P < 0.05$, $^{**}P < 0.01$, compared with the non-treated control; $^{\#}P < 0.05$, $^{\#\#}P < 0.01$, $^{\#\#\#}P < 0.001$ compared with TGF-β1 (1 ng·mL^{-1})-treated cells

transdifferentiation in NRK-49F and tubular cells of rat kidney into myofibroblasts could be effectively prevented by treatment with AS-IV.

CTGF may function as a chaperone to modify the conformation or solubility of TGF-β1 and thus facilitate TGF-β binding to type II TGF-β receptor.[35] Recent evidences indicate that CTGF expressed in the tubular epithelium plays a pivotal role in TGF-β-dependent renal fibrogenesis,[36] because CTGF is a downstream mediator of TGF-β signaling.[37] This supported by the findings that blockade of CTGF by antisense strategy or application fluorofenidone is able to attenuate renal fibrosis in obstructive nephropathy,[38,39] and mediated tubular EMT induced by TGF-β, and advanced glycation end products.[40,41] Our study demonstrated that AS-IV reduced enhancement of CTGF expression in UUO-induced renal fibrosis and decreased TGF-β1 caused CTGF expression in dose-dependent manners, suggesting that AS-IV may attenuate renal fibrosis via reducing CTGT expression.

The fibronectin and collagen I and III are major ECM proteins that serve as a scaffold for deposition of other proteins. Furthermore, fibronectin functions as a fibroblast chemoattractant and promotes their differentiation, which may be a crucial phenomenon in the pathogenesis of tubulointerstitial fibrosis.[42] As shown in Figures 4 and 6, treatment with AS-IV significantly reduced the expression of fibronectin and type I, III collagen in UUO-induced renal fibrosis and TGF-β1-stimulated fibronectin and type I, III collagen expression in dose-dependent manners. These findings suggest that blocking of TGF-β signaling pathway by AS-IV is sufficient to prevent the generation of ECM components.

Recent studies indicate that specific targeting the downstream TGF-β/Smad3 signaling pathway by overexpression of Smad7, rather than blocking the general effect of TGF-β1, may represent a specific and effective therapeutic strategy for kidney diseases.[43] Now, it is clear that overexpression of Smad7 in the nucleus could export Smad7 to the cytoplasm,[44] and transported to the plasma membrane, leading to inhibition of TGF-β signaling by degradation of the type I TGF-β receptor where it inhibits Smad2/3 activation.[9,45] In the present study, we found that UUO-induced renal fibrosis was associated with a significant activation of Smad2/3 but loss of Smad7, and consistent to the observation in cultured NRK-49F cells stimulated by TGF-β1. Furthermore, knockdown of Smad7 in cultured NRK-49F cells increased a TGF-β1-stimulated Smad2/3 phosphorylation, and subsequently induced EMT and the expression of ECM proteins. Those observations suggest that disruption of negative feedback loop between Smad7 and Smad 2/3 signaling could be important in the pathogenesis of renal fibrosis. This is confirmed by recent studies that the disruption of *Smad7* gene or down-regulation of Smad7 expression contributes to renal fibrosis in obstructive nephropathy.[7,12] Notably, previous research showed that Smad2 may function to inhibit Smad3-mediated ECM production and fibrosis by competitively inhibiting Smad3 phosphorylation, nuclear translocation, transcriptional activity, and the binding to the target genes.[46] In contrast, the present study demonstrated that treatment with AS-IV can

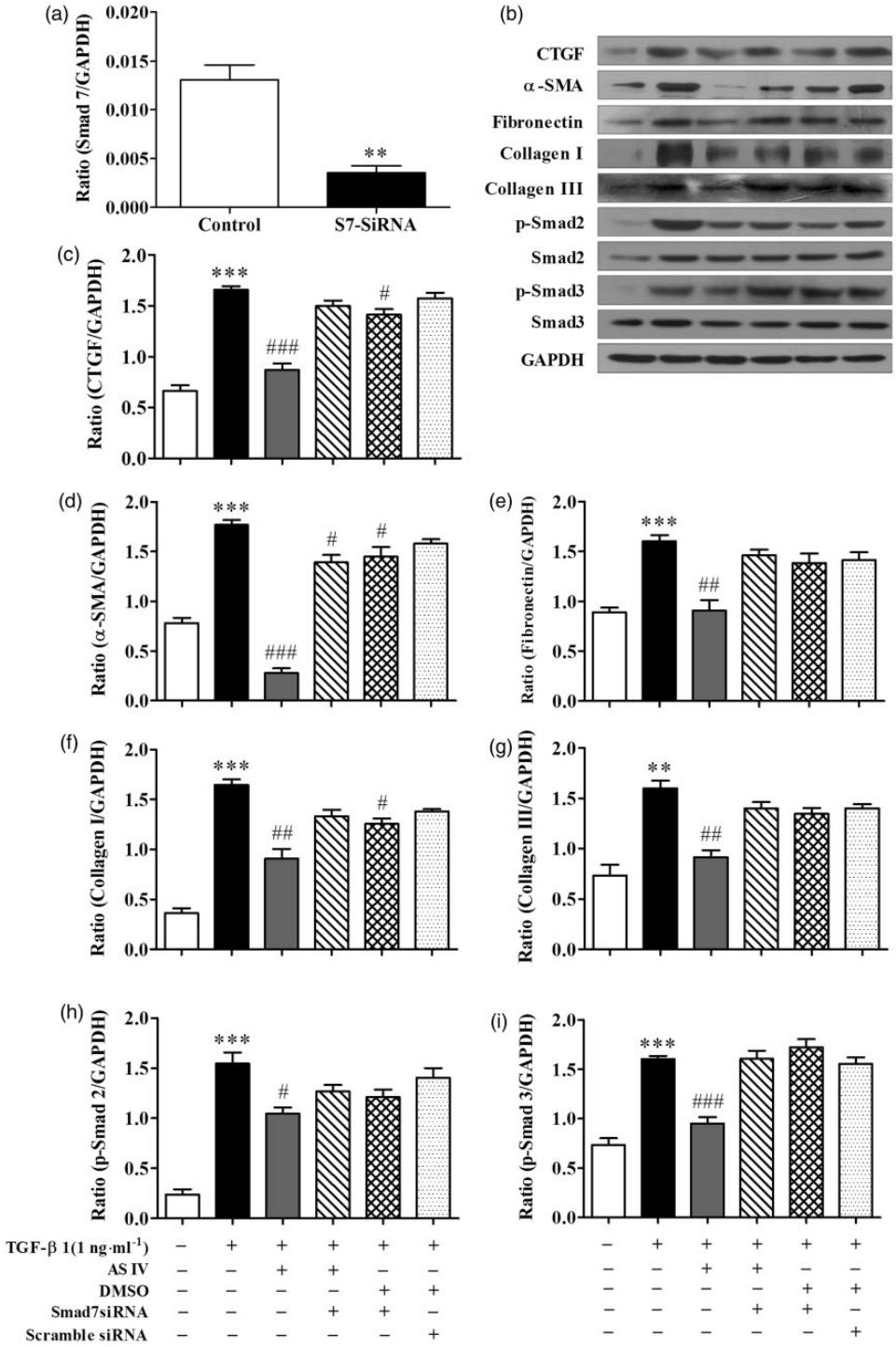

Figure 11 Knockdown of Smad7 in NRK-49 F cells prevents the inhibitory effect of AS-IV on TGF-β-induced renal fibrosis. (A) Real-time PCR shows reduction of Smad7 mRNA by siRNA technique. (B) Western blot shows that knockdown of Smad7 in NRK-49 F results in a loss of AS-IV (40 μM)-induced inhibition of TGF-β1 (1 ng·mL^{-1})-mediated CTGF, α-SMA, fibronectin, collagen I, III, p-Smad2, and p-Smad3 expression at 24 h. (C–I) Summary histogram showing the relative protein expression ratio from experiments similar to those shown in B. Data represent mean ± SEM for at least three independent experiments. $^{*}P < 0.05$, $^{***}P < 0.001$, compared with non-treated control; $^{\#}P < 0.05$, $^{\#\#}P < 0.01$, $^{\#\#\#}P < 0.001$ compared with TGF-β1 (1 ng·mL ^{1})-treated cells

dose-dependently inhibit the TGF-β/Smad signaling pathways via suppressing TGF-β1 expression, down-regulate Smad2/3 phosphorylation, and induce Smad7 expression in UUO-induced renal fibrosis, and AS-IV can suppress TGF-β1 stimulated Smad2/3 phosphorylation and up-regulate Smad7 expression in cultured NRK-49F cells. These results suggest that induction of Smad7, but not Smad2, thereby restoring the imbalance between TGF-β/Smad signaling, may be a key mechanism by which AS-IV attenuated UUO-induced renal fibrosis *in vivo* and

TGF-β1-stimualted EMT and ECM deposition *in vitro*. This concern was further extended by finding that knockdown of *Smad7* gene in NRK-49F cells was able to prevent AS-IV-induced inhibition of Smad2/3 signaling activation, EMT, and the expression of ECM proteins in response to TGF-β1.

In conclusion, the current study found that treatment with AS-IV has mild renoprotective efficacy in renal interstitial fibrosis, which is sometimes close to the effect of enalapril. The understanding mechanism by which AS-IV-treated chronic renal disease associated fibrosis is closely related to induction of Smad7, thereby inhibiting TGF-β/Smad signaling.

Author contributions: XMZ, WP and HC participated in its design and coordination, and evaluated the statistical analysis and critically revised the manuscript and guaranteed of intergrity of the entire study. LW, YFC, and ZTY carried out the experiment. WCZ and PHY performed statistical analysis and edit the manuscript. LW was involved in designing the study and drafting the manuscript. All authors read and approved the final manuscript.

ACKNOWLEDGMENTS

This work was supported by General Medicine of Key Discipline Construction Project, State Administration of Traditional Chinese Medicine of the People's Republic of China; Leading Academic Discipline Project of State Administration of Traditional Chinese Medicine of China, Talent Project of Integrative Medicine of Shanghai Municipal Health Bureau (ZYSNXD012-RC-ZXY); Key Medical Discipline Project of Shanghai Municipal Health Bureau (ZK2012A34); Independent Innovation Research Fund of Putuo District Science and Technology Committee (2012PTKW002) and Department of Veteran Affairs MERIT Award (5I01BX000994).

REFERENCES

1. Chatziantoniou C, Dussaule JC. Insights into the mechanisms of renal fibrosis: is it possible to achieve regression? *Am J Physiol Renal Physiol* 2005;**289**:F227–34
2. Li R, Wang Y, Liu Y, Chen Q, Fu W, Wang H, Cai H, Peng W, Zhang X. Curcumin inhibits transforming growth factor-beta1-induced EMT via PPARgamma pathway, not Smad pathway in renal tubular epithelial cells. *PLoS One* 2013;**8**:e58848
3. Zeisberg M, Kalluri R. The role of epithelial-to-mesenchymal transition in renal fibrosis. *J Mol Med (Berl)* 2004;**82**:175–81
4. Zeisberg M, Neilson EG. Mechanisms of tubulointerstitial fibrosis. *J Am Soc Nephrol* 2010;**21**:1819–34
5. Yang J, Liu Y. Dissection of key events in tubular epithelial to myofibroblast transition and its implications in renal interstitial fibrosis. *Am J Pathol* 2001;**159**:1465–75
6. Liu N, Tolbert E, Pang M, Ponnusamy M, Yan H, Zhuang S. Suramin inhibits renal fibrosis in chronic kidney disease. *J Am Soc Nephrol* 2011;**22**:1064–75
7. Fukasawa H, Yamamoto T, Togawa A, Ohashi N, Fujigaki Y, Oda T, Uchida C, Kitagawa K, Hattori T, Suzuki S, Kitagawa M, Hishida A. Down-regulation of Smad7 expression by ubiquitin-dependent degradation contributes to renal fibrosis in obstructive nephropathy in mice. *Proc Natl Acad Sci U S A* 2004;**101**:8687–92
8. Schnaper HW, Hayashida T, Poncelet AC. It's a Smad world: regulation of TGF-beta signaling in the kidney. *J Am Soc Nephrol* 2002;**13**:1126–8
9. Ebisawa T, Fukuchi M, Murakami G, Chiba T, Tanaka K, Imamura T, Miyazono K. Smurf1 interacts with transforming growth factor-beta type I receptor through Smad7 and induces receptor degradation. *J Biol Chem* 2001;**276**:12477–80
10. Kavsak P, Rasmussen RK, Causing CG, Bonni S, Zhu HT, Thomsen GH, Wrana JL. Smad7 binds to Smurf2 to form an E3 ubiquitin ligase that targets the TGF beta receptor for degradation. *Mol Cell* 2000;**6**:1365–75
11. Nakao A, Afrakhte M, Moren A, Nakayama T, Christian JL, Heuchel R, Itoh S, Kawabata M, Heldin NE, Heldin CH, ten Dijke P. Identification of Smad7, a TGFbeta-inducible antagonist of TGF-beta signalling. *Nature* 1997;**389**:631–5
12. Chung ACK, Huang XR, Zhou L, Heuchel R, Lai KN, Lan HY. Disruption of the Smad7 gene promotes renal fibrosis and inflammation in unilateral ureteral obstruction (UUO) in mice. *Nephrol Dial Transpl* 2009;**24**:1443–54
13. Liu GX, Li YQ, Huang XR, Wei L, Chen HY, Shi YJ, Heuchel RL, Lan HY. Disruption of Smad7 promotes ANG II-mediated renal inflammation and fibrosis via Sp1-TGF-beta/Smad3-NF-kappaB-dependent mechanisms in mice. *PLoS One* 2013;**8**:e53573
14. Lan HY, Mu W, Tomita N, Huang XR, Li JH, Zhu HJ, Morishita R, Johnson RJ. Inhibition of renal fibrosis by gene transfer of inducible Smad7 using ultrasound-microbubble system in rat UUO model. *J Am Soc Nephrol* 2003;**14**:1535–48
15. Li JH, Zhu HJ, Huang XR, Lai KN, Johnson RJ, Lan HY. Smad7 inhibits fibrotic effect of TGF-beta on renal tubular epithelial cells by blocking Smad2 activation. *J Am Soc Nephrol* 2002;**13**:1464–72
16. Liu SF, Chang SY, Lee TC, Chuang LY, Guh JY, Hung CY, Hung TJ, Hung YJ, Chen PY, Hsieh PF, Yang YL. Dioscorea alata attenuates renal interstitial cellular fibrosis by regulating Smad- and epithelial-mesenchymal transition signaling pathways. *PLoS One* 2012;**7**:e47482
17. Tang LX, He RH, Yang G, Tan JJ, Zhou L, Meng XM, Huang XR, Lan HY. Asiatic acid inhibits liver fibrosis by blocking TGF-beta/Smad signaling *in vivo* and *in vitro*. *PLoS One* 2012;**7**:e31350
18. Qiu LH, Xie XJ, Zhang BQ. Astragaloside IV improves homocysteine-induced acute phase endothelial dysfunction via antioxidation. *Biol Pharm Bull* 2010;**33**:641–6
19. Zhao J, Yang PY, Li F, Tao L, Ding H, Rui YC, Cao ZW, Zhang WD. Therapeutic effects of astragaloside IV on myocardial injuries: multi-target identification and network analysis. *PLoS One* 2012;**7**:e44938
20. Gui D, Huang J, Guo Y, Guo J, Chen Y, Xiao W, Liu X, Wang N. Astragaloside IV ameliorates renal injury in streptozotocin-induced diabetic rats through inhibiting NF-kappaB-mediated inflammatory genes expression. *Cytokine* 2013;**61**:970–7
21. Gui D, Huang J, Liu W, Guo Y, Xiao W, Wang N. Astragaloside IV prevents acute kidney injury in two rodent models by inhibiting oxidative stress and apoptosis pathways. *Apoptosis* 2013;**18**:409–22
22. Tan SF, Wang GF, Guo YP, Gui DK, Wang NS. Preventive effects of a natural anti-inflammatory agent, astragaloside IV, on ischemic acute kidney injury in rats. *Evid-Based Complement Altern* 2013;**2013**:284025
23. Zheng R, Deng YY, Chen YP, Fan JM, Zhang MH, Zhong YF, Zhu R, Wang L. Astragaloside IV attenuates complement membranous attack complex induced podocyte injury through the MAPK pathway. *Phytother Res* 2012;**26**:892–8
24. Gui DK, Guo YP, Wang F, Liu W, Chen JG, Chen YF, Huang JH, Wang N. Astragaloside IV, a novel antioxidant, prevents glucose-induced podocyte apoptosis *in vitro* and *in vivo*. *PLoS One* 2012;**7**:e39824
25. Qi W, Niu J, Qin Q, Qiao Z, Gu Y. Astragaloside IV attenuates glycated albumin-induced epithelial-to-mesenchymal transition by inhibiting oxidative stress in renal proximal tubular cells. *Cell Stress Chaperon.* Epub ahead of print 2013
26. Meng LQ, Tang JW, Wang Y, Zhao JR, Shang MY, Zhang M, Liu SY, Qu L, Cai SQ, Li XM. Astragaloside IV synergizes with ferulic acid to inhibit renal tubulointerstitial fibrosis in rats with obstructive nephropathy. *Br J Pharmacol* 2011;**162**:1805–18
27. Ikezumi Y, Suzuki T, Hayafuji S, Okubo S, Nikolic-Paterson DJ, Kawachi H, Shimizu F, Uchiyama M. The sialoadhesin (CD169) expressing a macrophage subset in human proliferative glomerulonephritis. *Nephrol Dial Transpl* 2005;**20**:2704–13
28. Huang LH, Haylor JL, Hau Z, Jones RA, Vickers ME, Wagner B, Griffin M, Saint RE, Coutts IGC, El Nahas AM, Johnson TS.

Transglutaminase inhibition ameliorates experimental diabetic nephropathy. *Kidney Int* 2009;**76**:383–94
29. Li Y, Sun Y, Liu F, Sun L, Li J, Duan S, Liu H, Peng Y, Xiao L, Liu Y, Xi Y, You Y, Li H, Wang M, Wang S, Hou T. Norcantharidin inhibits renal interstitial fibrosis by blocking the tubular epithelial-mesenchymal transition. *PLoS One* 2013;**8**:e66356
30. Park SH, Choi MJ, Song IK, Choi SY, Nam JO, Kim CD, Lee BH, Park RW, Park KM, Kim YJ, Kim IS, Kwon TH, Kim YL. Erythropoietin decreases renal fibrosis in mice with ureteral obstruction: role of inhibiting TGF-beta-induced epithelial-to-mesenchymal transition. *J Am Soc Nephrol* 2007;**18**:1497–507
31. Fragiadaki M, Mason RM. Epithelial-mesenchymal transition in renal fibrosis¯ evidence for and against. *Int J Exp Pathol* 2011;**92**:143–50
32. Moon JA, Kim HT, Cho IS, Sheen YY, Kim DK. IN-1130, a novel transforming growth factor-beta type I receptor kinase (ALK5) inhibitor, suppresses renal fibrosis in obstructive nephropathy. *Kidney Int* 2006;**70**:1234–43
33. Bottinger EP, Bitzer M. TGF-beta signaling in renal disease. *J Am Soc Nephrol* 2002;**13**:2600–10
34. Liu Y. Epithelial to mesenchymal transition in renal fibrogenesis: pathologic significance, molecular mechanism, and therapeutic intervention. *J Am Soc Nephrol* 2004;**15**:1–12
35. Abreu JG, Ketpura NI, Reversade B, De Robertis EM. Connective-tissue growth factor (CTGF) modulates cell signalling by BMP and TGF-beta. *Nat Cell Biol* 2002;**4**:599–604
36. Phanish MK, Wahab NA, Colville-Nash P, Hendry BM, Dockrell ME. The differential role of Smad2 and Smad3 in the regulation of pro-fibrotic TGFbeta1 responses in human proximal-tubule epithelial cells. *Biochem J* 2006;**393**:601–7
37. Qi W, Twigg S, Chen X, Polhill TS, Poronnik P, Gilbert RE, Pollock CA. Integrated actions of transforming growth factor-beta1 and connective tissue growth factor in renal fibrosis. *Am J Physiol Renal Physiol* 2005;**288**:F800–9
38. Li BX, Tang YT, Wang W, Xie YY, Wang NS, Yuan QJ, Zhang FF, Peng ZZ, Hu GY, Tao LJ. Fluorofenidone attenuates renal interstitial fibrosis in the rat model of obstructive nephropathy. *Mol Cell Biochem* 2011;**354**:263–73
39. Yokoi H, Mukoyama M, Nagae T, Mori K, Suganami T, Sawai K, Yoshioka T, Koshikawa M, Nishida T, Takigawa M, Sugawara A, Nakao K. Reduction in connective tissue growth factor by antisense treatment ameliorates renal tubulointerstitial fibrosis. *J Am Soc Nephrol* 2004;**15**:1430–40
40. Chung AC, Zhang H, Kong YZ, Tan JJ, Huang XR, Kopp JB, Lan HY. Advanced glycation end-products induce tubular CTGF via TGF-beta-independent Smad3 signaling. *J Am Soc Nephrol* 2010;**21**:249–60
41. Zhang C, Meng X, Zhu Z, Liu J, Deng A. Connective tissue growth factor regulates the key events in tubular epithelial to myofibroblast transition in vitro. *Cell Biol Int* 2004;**28**:863–73
42. Yokoi H, Sugawara A, Mukoyama M, Mori K, Makino H, Suganami T, Nagae T, Yahata K, Fujinaga Y, Tanaka I, Nakao K. Role of connective tissue growth factor in profibrotic action of transforming growth factor-beta: a potential target for preventing renal fibrosis. *Am J Kidney Dis* 2001;**38**:S134–8
43. Lan HY. Smad7 as a therapeutic agent for chronic kidney diseases. *Front Biosci* 2008;**13**:4984–92
44. Itoh S, Landstrom M, Hermansson A, Itoh F, Heldin CH, Heldin NE, ten Dijke P. Transforming growth factor beta1 induces nuclear export of inhibitory Smad7. *J Biol Chem* 1998;**273**:29195–201
45. Suzuki C, Murakami G, Fukuchi M, Shimanuki T, Shikauchi Y, Imamura T, Miyazono K. Smurf1 regulates the inhibitory activity of Smad7 by targeting Smad7 to the plasma membrane. *J Biol Chem* 2002;**277**:39919–25
46. Meng XM, Huang XR, Chung AC, Qin W, Shao X, Igarashi P, Ju W, Bottinger EP, Lan HY. Smad2 protects against TGF-beta/Smad3-mediated renal fibrosis. *J Am Soc Nephrol* 2010;**21**:1477–87

(Received January 1, 2014, Accepted March 12, 2014)